Catalysis Today 176 (2011) 21–27

Contents lists available at ScienceDirect

Catalysis Today

journal homepage: www.elsevier.com/locate/cattod

$Cu/Zn_xAl_yO_z$ supported catalysts (ZnO: Al_2O_3 = 1, 2, 4) for methanol synthesis

Pawel Mierczynski*, Tomasz P. Maniecki, Karolina Chalupka, Waldemar Maniukiewicz, Wojciech K. Jozwiak

Technical University of Lodz, Institute of General and Ecological Chemistry, 90-924 Łódź, Zeromskiego 116, Poland

ARTICLE INFO

Article history:
Received 29 September 2010
Received in revised form 30 May 2011
Accepted 9 June 2011
Available online 14 July 2011

Keywords:
Copper catalysts
$ZnAl_2O_4$
Binary oxide
Methanol synthesis

ABSTRACT

The main goal of this work was determination of the dependence of the physicochemical properties of Cu/support catalysts (ZnO, Al_2O_3, $ZnAl_2O_4$, $ZnAlO_{2.5}$, $Zn_2AlO_{3.5}$) with their activity in methanol synthesis. The formation of spinel $ZnAl_2O_4$ structure during calcination process was proved by XRD technique. The mechanism of methanol synthesis was discussed. Activity tests show that the most active catalyst was system supported on binary oxide $ZnAl_2O_4$.

1. Introduction

Methanol is industrially produced from synthesis gas $CO/CO_2/H_2$ under rather low temperature and high pressure conditions over a ternary $CuO–ZnO–Al_2O_3$ catalysts [1]. During the last decades, CO_2 hydrogenation to CH_3OH has gained wide interest as a mean to contribute to reduction of CO_2 emissions. Furthermore the direct conversion of CO_2 and hydrogen to CH_3OH has already been demonstrated with higher selectivity than CO and lower reaction temperature [2]. However, there is still controversy concerning the mechanism of methanol synthesis [3,4]. Some authors claimed that carbon monoxide is the main source for methanol synthesis. But this viewpoint cannot explain the remarkable improvement of activity after CO_2 introduction [5]. Saussey [6] and Fujita [7] claimed that methanol synthesis carried out from CO and CO_2 hydrogenation has different mechanisms. Fujita thought that during methanol synthesis running form CO and H_2 mixture, zinc formate was formed first, followed by hydrogenated to zinc methoxy and then reacted with surface hydroxyl species to form methanol. Whereas, CO_2 hydrogenation lead to both zinc formate and copper formate formation on the catalyst surface, then these formates are hydrogenated to methoxide, and hydrolyzed to methanol. Qi Sun [8] suggested that methanol was formed directly from CO_2 hydrogenation both for CO_2 and for CO/CO_2 hydrogenation, and b-$HCOO^-$ species were the key intermediate. The rate-limiting step was hydrogenation of bidenate formates surface species.

Many studies and discussions about the role of copper during hydrogenation of CO or CO_2 are available in literature. Particle size, surface area, metallic copper surface area and composition of $Cu/ZnO/A1_2O_3$ catalyst are important factors influencing on the catalytic process. Chinchen et al. proposed a linear relationship between the catalytic activity in methanol synthesis and metallic copper surface area of the catalyst [9,10]. Fujitani et al. [11] reported that the activity of methanol synthesis from CO increases with the concentration of Cu^+ sites. The Cu^+ as well as Cu^0 could possibly be active species during methanol synthesis from CO_2, where carbonate, formate and methoxy spices may be intermediates.

Lavalley et al. [12] reported that methanol is formed via an active formate species adsorbed on metallic copper, which depends on the copper dispersion and the ability of the mixed oxide phases (Cu–ZnO) to generate and store active hydrogen.

Additionally, activity of copper based catalysts can be improved by mixtures of metal oxides MO_x (M: Cr, Zn, Al) which were usually produced by co-precipitation or impregnation methods. Catalysts containing these metal oxides have been found to be more active than the individual component [13–16]. In addition some transition metals have been used as promoters to modify the activity of $Cu–ZnO/Al_2O_3$ catalysts in methanol synthesis [16].

Various methods for $Cu/ZnO/A1_2O_3$ catalysts preparation which allow to achieve large copper surface, fine particle size and optimized compositions leading to high catalytic activity and selectivity of methanol synthesis through CO or/and CO_2 hydrogenation were investigated. Tanaka and co-workers [17] prepared Cu/ZnO catalyst from a solution of copper and zinc nitrates dissolved in ethylene

* Corresponding author. Tel.: +48 42631 31 25; fax: +48 42631 31 28.
E-mail address: mierczyn25@wp.pl (P. Mierczynski).

0920-5861/$ – see front matter © 2011 Elsevier B.V. All rights reserved.
doi:10.1016/j.cattod.2011.06.009

glycol. They found that the selectivity to methanol was highest when the ratio of Cu/ZnO was 1. Deng et al. [18] reported that catalytic activity of methanol synthesis through CO_2 hydrogenation increasing with increasing of the metallic surface area for $Cu/ZnO/Al_2O_3$ system until it reaches a maximum at Cu/ZnO = 8 and then decreases at higher molar ratio.

In the present work copper supported catalysts containing 20 wt.%. Cu (Al_2O_3, $ZnAl_2O_4$, $ZnAlO_{2.5}$, $Zn_2AlO_{3.5}$, ZnO) were prepared by conventional impregnation method. The main goal of this work was investigation the influence of support composition on the structure of the catalyst and its catalytic activity in methanol synthesis from CO_2/H_2. The physicochemical properties of the catalysts were examined by BET, XRD, DRIFT, TPR-H_2 methods. Catalytic activity test in methanol synthesis by CO_2 hydrogenation were carried out under elevated pressure (4 MPa) in fixed bed reactor.

2. Experimental

2.1. Catalysts preparation

Copper supported catalysts $Cu/Zn_xAl_yO_z$ were prepared by wet aqueous impregnation method. Binary oxides of $Zn_xAl_yO_z$ (molar ratio Zn: Al = 0.5, 1, 2) were prepared by co-precipitation. Aqueous solutions of 1 M zinc acetate and 1 M aluminium nitrate were mixed in appreciate quantity under vigorous stirring at 80 °C. A concentrated ammonia solution was then added by dropwise addition until the pH reached values between 10 and 11 and the mixtures were stirred for another 30 min. The resulting fine precipitates were washed two times in deionized water and then dried at 120 °C for 15 h and subsequently calcined for 3 h in air at 600, 700 and 900 °C, respectively. Choice of the first temperature calcinaion was prescribed by necessity of spinel structure creation and for removal of the acetate precursor from catalytic systems. Higher temperature calcination was imposed to investigate of the phase composition during the calcination process.

Metal phase (Cu) was introduced on support surface by wet impregnation method with an aqueous solution of its nitrate and then the supported catalysts were dried at 120 °C and finally calcined for 4 h in air at 400 °C for removal of nitrates and at 700 °C for elucidate the interaction between support and active phase. Copper loading was 20 wt.% in all cases.

2.2. Methods of catalysts characterization

2.2.1. Specific surface area and porosity (BET)

The specific surface area and porosity of the catalysts and their supports were determined with automatic sorptometer Sorptomatic 1900. Samples were prepared at 250 °C and 12 h evacuation followed by low temperature nitrogen adsorption–desorption measurements were carried out using BET, liquid N_2 method.

2.2.2. Temperature programmed reduction (TPR-H_2)

The TPR-H_2 measurements were carried out in an automatic TPR system AMI-1 in the temperature range 25–900 °C with linear heating rate 10 °C/min. Samples (weight about 0.1 g) were reduced in hydrogen stream (5% H_2–95% Ar) with the gas volume velocity of 40 cm^3 per minute. The hydrogen consumption was monitored by a thermal conductivity detector.

2.2.3. XRD measurements

Room temperature powder X-ray diffraction patterns were collected using a PANalytical X'Pert Pro MPD diffractometer in Bragg-Brentano reflecting geometry. Copper CuK_α radiation from a sealed tube was utilized. Data were collected in the range 5–90° 2θ with step 0.0167° and exposition per one step of 27 s. Due to the fact that raw diffraction data contain some noise, the background during the analysis was subtracted using Sonneveld, E.J. and Visser algorithm. The data was then smoothed using cubic polynomial. All calculations were done with X'Pert HighScore Plus computer program.

Table 1
BET surface area measurements and average pore size for supports: $ZnAl_2O_4$, $ZnAlO_{2.5}$, $Zn_2AlO_{3.5}$, Al_2O_3 and ZnO calcined 3 h in air at various temperatures.

Support	Calcination temperature (°C)	Specific surface area (m^2/g)	Average pore size (Å)
Al_2O_3	400	237	27
$ZnAl_2O_4$	600	63	30
$ZnAlO_{2.5}$	600	60	42
$Zn_2AlO_{3.5}$	600	19	55
ZnO	400	37	–

2.2.4. Diffuse reflectance infrared fourier transform spectroscopy (DRIFTS)

Infrared spectra were recorded with a Thermo Scientific Nicolet 6700 FTIR spectrometer equipped with a liquid nitrogen cooled MCT detector. Before analysis the sample was reduced at 300 °C in gas reduction mixture (5%H_2–95%Ar for 1 h). A resolution of 4.0 cm^{-1} was used throughout the investigation. 64 scans were taken to achieve a satisfactory signal to noise ration. The background spectrum was collected at 50 °C after reduction. Then the reduction mixture was shifted to a reaction mixture of approximately 20% CO_2 and 80% H_2. Reaction was carried out in temperature range 50–280 °C under atmospheric pressure. Spectra were taken in each temperature after 10 min in reaction mixture flow.

2.2.5. Catalytic activity test

Carbon dioxide hydrogenation tests were carried out in a fixed bed reactor using a gas mixture of H_2 and CO_2 with molar ratio 3:1, respectively. The process was carried out under elevated pressure (4 MPa) at 180 and 260 °C. Before activity tests, the catalysts were pre-reduced for 2 h in a flow of 5% H_2–95% Ar at 300 °C under atmospheric pressure. The catalysts were cooled to the reaction temperature of 260 °C and then the inlet flow was switched to reaction mixture. The steady-state activity measurements were taken after at least 12 h on the stream. The analysis of the reaction products were carried out by an on-line gas chromatograph equipped with FID detector and 10% Carbowax 1500 on Graphpac column. The CO and CO_2 concentrations were monitored by GC chromatograph equipped with TCD detector (120 °C, 130 mA), and Carbopshere 60/80 (90 °C) column. CO conversion was calculated by the following equation:

$$CO_2\ \text{conv.} = \left[\frac{(CO_2\ \text{in feed} - CO_2\ \text{in effluent})}{(CO_2\ \text{in feed})} \times 100\right]$$

The selectivity of the products were calculated as follows:

$$P_i\ \text{selectivity} = \left(\frac{P_i\ \text{yield}}{\sum P_i\ \text{yield}}\right) \times 100$$

P_i is the mol number of every product.

3. Results and discussion

The BET results embracing surface area and dominant pore size for the calcined at various temperature supports (Al_2O_3, ZnO, $ZnAl_2O_4$, $ZnAlO_{2.5}$, $Zn_2AlO_{3.5}$) are shown in Table 1. The individual Al_2O_3 calcined at 400 °C had the largest specific surface area of 237 m^2/g compared to the ZnO sample which had the lowest surface area of 37 m^2/g. The binary oxides $ZnAl_2O_4$ and $ZnAlO_{2.5}$ showed intermediate specific surface area of about 60 m^2/g. On the

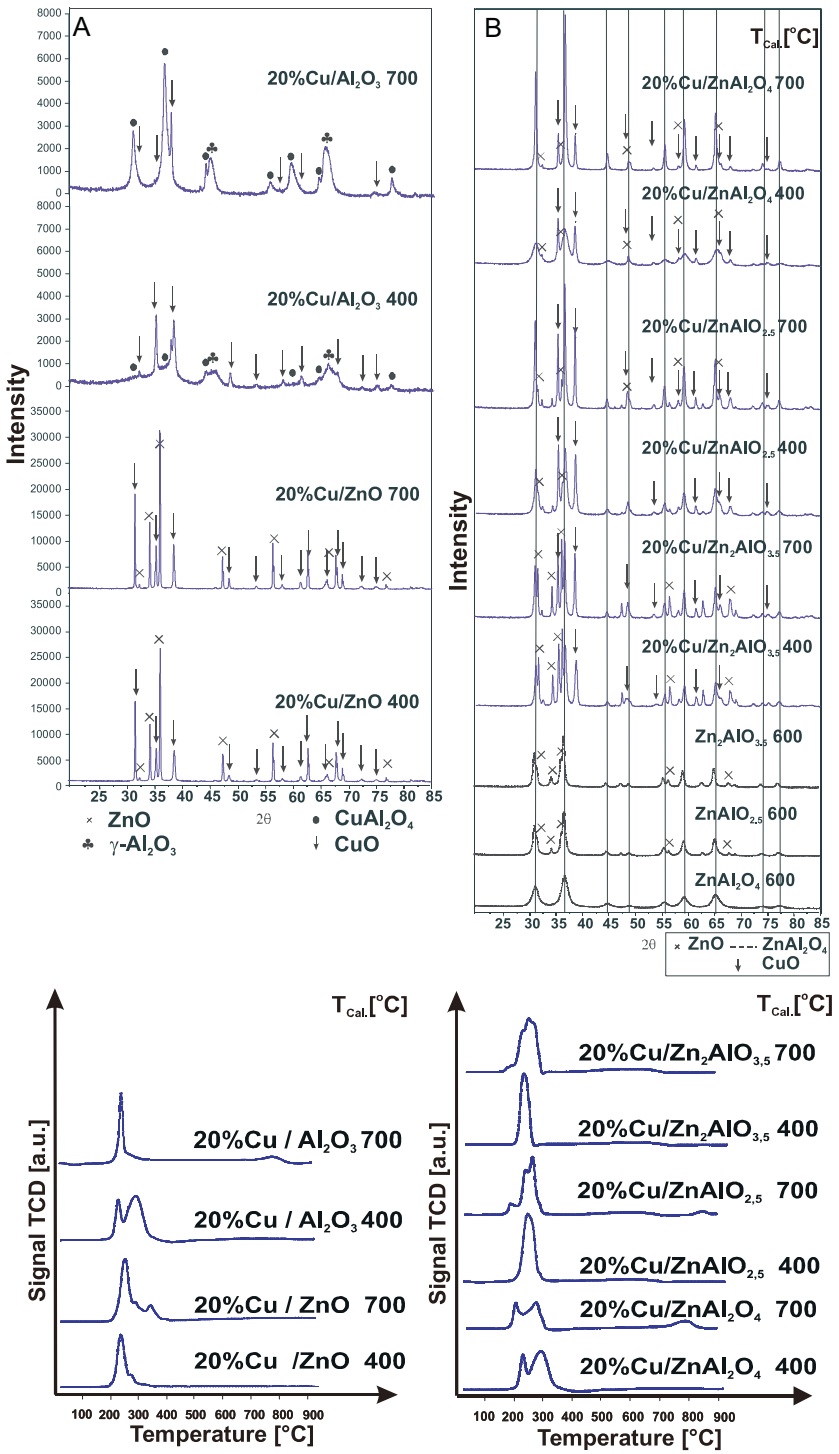

Fig. 1. (A) XRD patterns for Cu/Al_2O_3, Cu/ZnO catalysts calcined 400 and and 700 °C. (B) XRD patterns for binary oxides and copper catalysts 20%Cu/support (support–$ZnAl_2O_4$, $ZnAlO_{2.5}$, $Zn_2AlO_{3.5}$) calcined at 400 and 700 °C. (C) TPR profiles for copper supported catalysts supported on Al_2O_3 or ZnO. (D) TPR profiles for copper supported on binary oxides calcined at 400 and 700 °C.

contrary $Zn_2AlO_{3.5}$ had the smallest surface area in comparison to remaining binary oxides. This result can be explained by the largest content of zinc oxide entering in composition of this system (see Fig. 1B).

The X-ray patterns of binary oxides after calcinations at 600 °C and copper catalysts supported on different support calcined at 400 and 700 °C are shown in Fig. 1A and B, respectively. The XRD data for binary oxide $ZnAl_2O_4$ calcined at 600 and 700 °C confirmed the formation of spinel structure phase ($ZnAl_2O_4$). Increasing of the calcination temperature causes only growth of sample crystallization (see our previous work [19]). This indicated that all content of zinc converts into spinel structure (AB_2X_4 – the compounds related to $A^{II}B^{III}{}_2X_4$ system – where A – metal, B – three – valency element, X – halogen including oxygen [20]).

The diffractogrames recorded for $ZnAlO_{2.5}$ and $Zn_2AlO_{3.5}$ bioxides shows that in addition to $ZnAl_2O_4$ spinel structure, zinc oxide

phase was also detected (see Fig. 1B). It appears that the rest of zinc which did not convert into spinel structure exists as an individual phase. This fact can explain the lower specific surface area observed for $Zn_2AlO_{3.5}$ (see Table 1).

Diffraction curves recorded for copper catalysts supported on Al_2O_3 and ZnO are presented in Fig. 1A. On the difractograms of 20%Cu/Al_2O_3 catalyst calcined at 400 °C the presence of γ-Al_2O_3 and CuO as a major phase [21] and $CuAl_2O_4$ as a minor phase were detected. Increasing calcination temperature to 700 °C manifested sample crystallization and enlargement of $CuAl_2O_4$ phase. Copper aluminate $CuAl_2O_4$ phase is stable above 600 °C [22], which is confirmed by our results, showing that in the case of 20%Cu/Al_2O_3 catalyst calcined at 700 °C $CuAl_2O_4$ spinel structure was a major phase.

XRD measurements carried out for 20%Cu/ZnO show that only zinc and copper oxides phases are present. Increasing temperature of calcination causes only catalyst crystallization.

Diffraction curves recorded for 20 wt.%. Cu catalysts supported on binary oxides show zinc oxide, copper oxide and spinel $ZnAl_2O_4$ structure phases (see Fig. 1B). In the case of catalysts calcined at 700 °C the formation of $CuAl_2O_4$ spinel structure by substitution of zinc ions by copper ions in the $ZnAl_2O_4$ structure by increasing of the zinc oxide phase content was confirmed.

Two spinel phases $ZnAl_2O_4$ and $CuAl_2O_4$ are isostructural and distinction of these phases in the same sample by XRD technique is rather impossible due to reflexes display nearly coincident in their diffraction patterns [23].

The reducibility of catalysts was examined by temperature programmed reduction. TPR profiles of copper supported catalysts are shown in Fig. 1C and D. For 20%Cu/Al_2O_3 supported catalysts (see Fig. 1C) we observed two or three reduction stages which depend on calcination temperature. Two overlapped TPR profiles situated at lower temperature are attributed to copper oxides reduction ($CuO \rightarrow Cu_2O \rightarrow Cu$) [24]. For catalyst calcined at 700 °C hydrogen consumption peak observed at about 760 °C is assigned to spinel phase $CuAl_2O_4$ reduction which was also visible in the XRD pattern recorded for 20%Cu/Al_2O_3 after calcination at 700 °C (see Fig. 1A).

TPR profiles recorded for copper catalysts supported on ZnO shows two partially resolved reduction effects as well as for 20%Cu/Al_2O_3 system calcined at 400 °C. These reduction stages are connected with copper oxides reduction ($CuO \rightarrow Cu_2O \rightarrow Cu$).

Similar results were obtained by Pettersson and co-workers [25] who studied Cu/ZnO catalysts impregnated on γ-Al_2O_3. They reported that the reduction of CuO proceeds stepwise ($Cu^{2+} \rightarrow Cu^{+} \rightarrow Cu^{0}$) judging from the TPR results. Turco et al. [26] also confirmed easy reduction of Cu^{2+} to Cu^{+} and Cu^{0} in the case of CuO/ZnO/Al_2O_3 catalyst.

Wang et al. [27] investigated the reduction of Cu/γ-Al_2O_3 catalysts and suggested that when Cu content is low (5%Cu wt.) only one reduction peak (α) is observed in the TPR patterns. However, with increasing the Cu content additional reduction peak (β) appears. They claimed that the first peak α represents the reduction of highly dispersed copper oxide, the second peak β was assigned to the reduction of CuO crystal phase.

TPR profiles of copper catalysts supported on binary oxides (see Fig. 1D) show one, two or three regions of hydrogen consumption depending on catalysts composition and calcination temperature. At low reduction temperature we observed one or two reduction stages for all catalysts. These reduction effects are connected with copper oxide reduction directly to metallic copper or through reduction of CuO to Cu_2O as an intermediately stage. However, high temperature reduction effect observed in the case of copper catalyst supported on $ZnAl_2O_4$, $ZnAlO_{2,5}$ catalysts after calcination at 700 °C is connected with $CuAl_2O_4$ structure reduction. Whereas, 20%Cu/$Zn_2AlO_{3.5}$ catalyst reduces in one stage and this stage is attributed to copper oxides reduction. The presence of high reduction effect and growth of zinc oxide phase content on the diffractograms of 20%Cu/$ZnAl_2O_4$, 20%Cu/$ZnAlO_{2,5}$ catalysts calcined at 700 °C suggest that $CuAl_2O_4$ phase is formed by substitution of zinc ions by copper ions in the $ZnAl_2O_4$ structure [19].

Fig. 2 shows the part of the IR spectra obtained in flowing CO_2/H_2 reaction mixture under atmospheric pressure in the temperature range 50–280 °C for copper catalysts supported on binary oxides. Many authors [28–33] claim that the formate and carbonate species were formed when Cu-based catalyst was exposed to CO_2/H_2 or $CO/CO_2/H_2$ at low temperatures. The hydrogenation of carbonate species to formate species was proved in several reports [33–36]. Our studies show that during temperature programmed reaction, a change of species adsorbed on the catalyst surface was observed. An IR spectrum showed that copper formate (HCOO–Cu: 2925, 2850, 1620, 1364, 1350 cm^{-1}), zinc formate (HCOO–Zn: 2970, 2880, 2700, 1591, 1372, 1365 cm^{-1}) carbonate (CO_3^{2-}: 1620, 1570–1440, 1220 cm^{-1}), zinc methoxide (CH_3O–Zn: 2935, 2825, 1060 cm^{-1}) and gaseous CO (CO: 2118, 2171 cm^{-1}) were formed in the course of the CO_2–H_2 during growth of temperature of reaction [37–39]. At the beginning of reaction from 50 to 120 °C we can easily distinguish only carbonate species (CO_3^{2-}: 1620, 1570–1440, 1220 cm^{-1}). These carbonate species are formed by the reaction of CO_2 or CO (CO comes from dissociative adsorption of CO_2 with hydroxyl group situated on metal [37,38], which are further hydrogenated to more stable monodentate or bidentate formate species at higher temperature. Starting at 160 °C can be observed methoxy species formation. However, very interesting result observed for all catalysts was the fact that appearance of methoxy species was accompanied with growth of b-formates intensity bands on the spectrum and these species disappeared during the reaction evidenced by decreasing intensity of the band assigned to b-$HCOO_s^-$ species. This observation can suggest that bidentate formates are directly hydrogenated to methanol through methoxy species and the main intermediate species during methanol synthesis are b-$HCOO^-$ groups, and this is the stage of the reaction which determines the rate of methanol synthesis. It is noteworthy that the hydrogenation of b-$HCOO_s^-$ species is greater than that of monodentate formate species [35].

The results above are in agreement with previous reports [37,40,41] which described that methanol was formed directly from CO_2 hydrogenation both for CO_2 and CO/CO_2 hydrogenation and also confirmed that b-$HCOO^-$ species is the key intermediate for methanol synthesis and hydrogenation of this species is the rate-limiting step of the reaction.

The influence of different support on the activity of copper catalysts in methanol synthesis was also studied in this work. The temperature characteristics of catalytic activity of copper supported catalysts in hydrogenation of CO_2 expressed in g $CH_3OH\,g^{-1}$ cat. h^{-1} are presented in Fig. 3. The results of CO_2 conversion and selectivity of methanol synthesis reaction carried out at 180 and 260 °C by using Cu/Al_2O_3, Cu/$Zn_xAl_yO_z$, Cu/ZnO catalysts with 20 wt.%Cu loading are presented in Table 2. It is evident that the CO_2 conversion increases with increasing of the reaction temperature. The methanol yield increases with growth of reaction temperature and the molar ratio between Cu and ZnO (see Fig. 3). The highest yield of methanol formation was observed in the case of 20%Cu/$ZnAl_2O_4$ for which Cu/ZnO was equal 0.72.

The lowest yield and selectivity to methanol was found for the 20%Cu/ZnO catalysts. Very similar selectivity demonstrated 20%Cu/$Zn_2AlO_{3.5}$ system with Cu/ZnO = 0.43. Intermediate yield was shown Cu/$ZnAlO_{2.5}$ catalyst. These results suggest that Cu–Zn site are the active sites in methanol synthesis. The Cu/$ZnAl_2O_4$

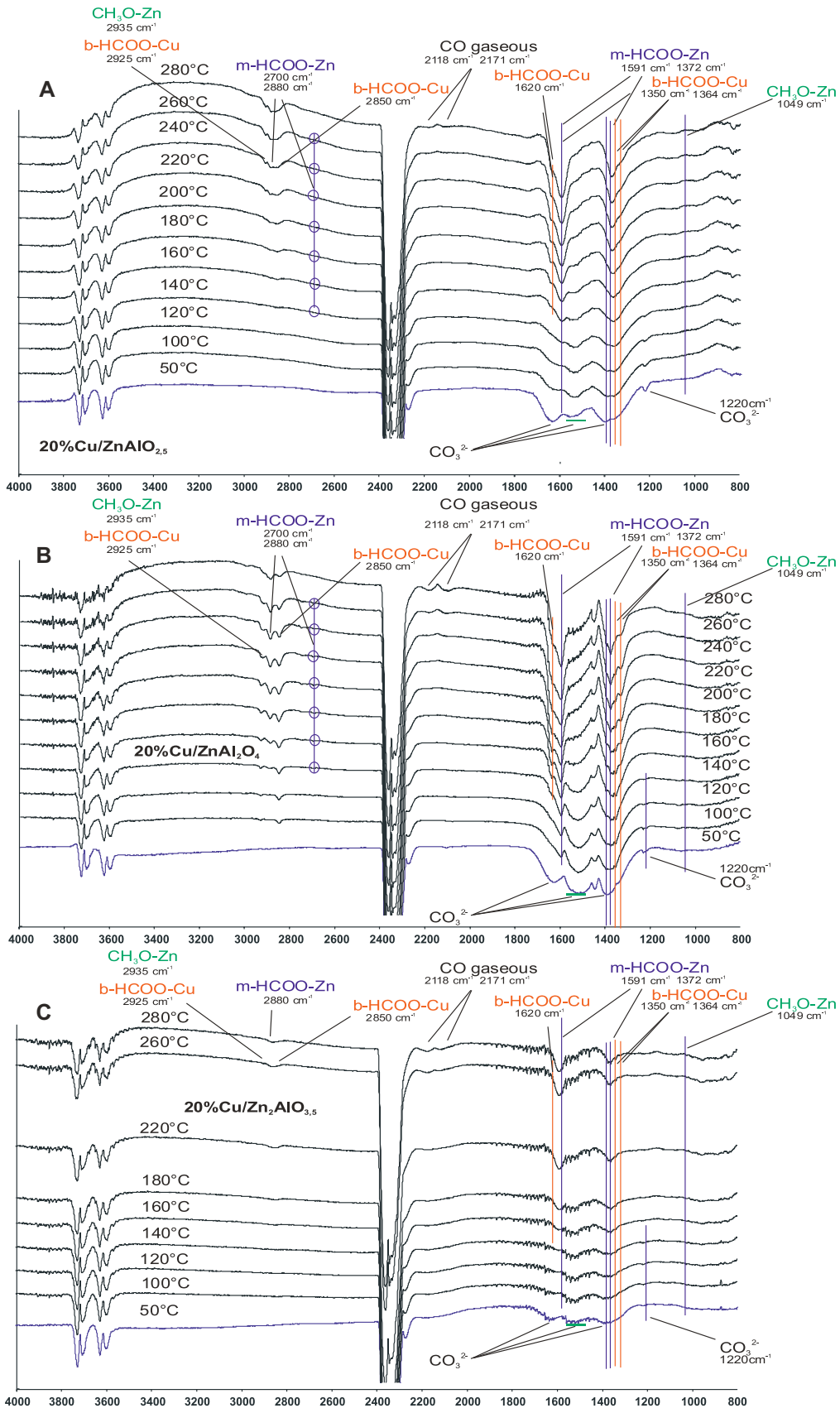

Fig. 2. DRIFT spectra for methanol synthesis from CO_2/H_2 recorded during temperature – programmed – reaction under atmospheric pressure for 20%Cu/support catalysts (support = $ZnAl_2O_4$, $ZnAlO_{2.5}$, $Zn_2AlO_{3.5}$).

Table 2
The reaction results for methanol synthesis from CO_2/H_2 with various $Cu/Zn_xAl_yO_z$ catalysts.

Catalyst	CO_2 Conversion (%)		Selectivity									
			CO (%)		CH_4 (%)		MeOH (%)		C_2+ (%)		DME (%)	
			Temperature (°C)									
	180	260	180	260	180	260	180	260	180	260	180	260
$20\%Cu/Al_2O_3$	4	8	51	53	0.5	0.1	48.5	46.8	–	0.1	–	–
$20\%Cu/ZnAl_2O_4$	4	10	17	25	3	3	79	70	–	1	1	1
$20\%Cu/ZnAlO_{2.5}$	3	8	16	18	2	2	82	76	–	4	–	–
$20\%Cu/Zn_2AlO_{3.5}$	5	11	13	9	0.2	0.3	5	2	81.8	88.7	–	–
20%Cu/ZnO	4	12	25	19	6	2	4	1	65	78	–	–

Reaction condition: weight of catalyst = 2 g, H_2/CO_2 ratio in the feed = 3, temperature = 180 and 260 °C, total pressure = 4 MPa.

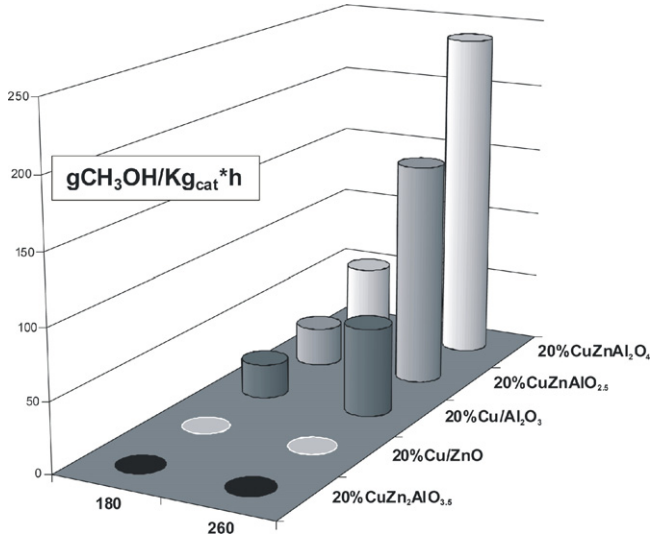

Fig. 3. Influence of different support on activity of copper supported catalysts after calcination at 400 °C.

catalyst having the highest Cu/ZnO molar ratio, and thus highest quantity of $CuAl_2O_4$ is created during calcinations process. This is confirmed by the intensity of high temperature reduction effect visible in the TPR profile of $20\%Cu/ZnAl_2O_4$ after calcinations at 700 °C (see Fig. 1D). The fact that methanol synthesis are exothermic reaction caused that highest conversions – and thus the highest methanol yield – are obtained at low temperatures and high pressures. As it was possible to expect the selectivity of copper supported catalysts decrease with increasing of reaction temperature. This is due to the limitation of methanol synthesis reaction equilibrium, because increasing temperature disadvantages methanol formation. In distinguishing from methanol selectivity, the yield of other products (CH_4, CO, C_{2+}, DME) grow with increasing reaction temperature, which is responsible for continuously increasing CO_2 conversion and decreasing selectivity to methanol at high temperature.

4. Conclusions

1. XRD and TPR results confirmed the formation of $CuAl_2O_4$ spinel phase during calcination in the case of $20\%Cu/Al_2O_3$. Remaining above conclusion, high temperature reduction effect located in the same temperature range as for Cu/Al_2O_3 system indicated also copper aluminate formation for $Cu/Zn_xAl_yO_z$ systems.
2. The catalytic activity depends on the kind of support which is used in methanol synthesis. The highest activity showed catalyst supported on $ZnAl_2O_4$ bioxide (Zn/Al = 0.5 and Cu/ZnO = 0.72).
3. The b-$HCOO^-$ group formation from hydrogenation of carbonate surface species as a intermediate of methanol synthesis was proven. Disappearance of the methoxy group together with b-$HCOO^-$ species confirmed the proposed mechanism that the key stage of the reaction is hydrogenation of bidentate formate to methoxy species and finally to main product – methanol.

Acknowledgements

The financial support of this work by the Polish Scientific Research Council supports (Grant No. N N209 011234) is gratefully acknowledged.

References

[1] R. Yang, X. Yu, Y.I. Zhang, Wenze Li, Noritatsu Tsubaki, Fuel 87 (2008) 443.
[2] R. Raudaskoski, E. Turpeinen, R. Lenkkeri, E. Pongrácz, R.L. Keiski, Catal. Today 144 (2009) 318.
[3] T. Inui, H. Hara, M. Takeguchi, J.B. Kim, Catal. Today 36 (1997) 25.
[4] M. Saito, T. Fujitani, M. Takeuchi, T. Watanabe, Appl. Catal. A 138 (1996) 311.
[5] Xiaojuan Wang, Haipeng Zhang, Wei Li, Korean J. Chem. Eng. 27 (4) (2010) 1093.
[6] J. Saussey, J.C. Lavalley, J. Mol. Catal. 50 (1989) 343.
[7] S.I. Fujita, M. Usui, H. Ito, N. Takezawa, J. Catal. 157 (1995) 403.
[8] Q. Sun, C.W. Liu, W. Pan, Q.M. Zhu, J.F. Deng, Appl. Catal. A 171 (1998) 301.
[9] G.C. Chinchen, M.S. Spencer, K.C. Waugh, D.A. Whan, J. Chem. Soc. Faraday Trans. 83 (1987) 2193.
[10] G.C. Chinchen, K.C. Waugh, D.A. Whan, Appl. Catal. 25 (1986) 101.
[11] T. Fujitani, M. Saito, Y. Kanai, T. Kakumoto, T. Watanabe, J. Nakamura, T. Uchijima, Catal. Lett. 25 (1994) 271.
[12] F. Le Peltier, P. Chaumette, A. Kiennemann, J. Saussey, J.C. Lavalley, J. Chim. Phys. 93 (1996) 1376.
[13] T. Shisido, M. Yamamoto, D.L. Li, Y. Tian, H. Morioka, M. Honda, T. Sanko, K. Takehira, Appl. Catal. A: Gen. 303 (2006) 62.
[14] M. Saito, T. Fujitani, M. Takeuchi, T. Watanabe, Appl. Catal. A 138 (1996) 311–318.
[15] M. Saito, T. Fujitani, I. Takahara, T. Watanabe, M. Takeuchi, Y. Kanai, K. Moriya, T. Kakumoto, Energy Convers. Manage. 36 (1995) 577.
[16] Y. Nitta, O. Suwata, Y. Ikeda, Y. Okamoto, T. Imanaka, Catal. Lett. 26 (1994) 345.
[17] Y. Tanaka, Ch. Kawanura, A. Ueno, Y. Kotera, K. Takeuchi, Y. Sugi, Appl. Catal. 8 (1983) 325.
[18] J.F. Deng, Q. Sun, Y.L. Zhang, D. Wu, S.Y. Chen, Appl. Catal. A 139 (1996) 75.
[19] T.P. Maniecki, P. Mierczynski, K. Bawolak-Olczak, W. Maniukiewicz, W.K. Jozwiak, Polish J. Environ. Stud. 18 (No.1B) (2009) 120.
[20] A.S. Korotkov, N.M. Alexandrov, Comput. Mater. Sci. 35 (2006) 442.
[21] J. Sang Chai Kim, Hazard. Mater. B91 (2002) 285.
[22] F. Meyer, R. Hepelmann, S. Mathur, M. Veith, J. Mater. Chem. 9 (1999) 1755.
[23] M.N. Barroso, M.F. Gomez, J.A. Gamboa, L.A. Arrua, M.C. Abello, J. Phys. Chem. Solids 67 (2006) 1583.
[24] M. Ferrandom, J. Carno, S. Jaras, E. Bjornbom, Appl. Catal. A 180 (1999) 141.
[25] B. lindström, L.J. Pettersson, P.G. Menon, Appl. Catal. A 234 (2002) 111.
[26] M. Turco, G. Bagnasco, U. Constantino, F. Marmottini, T. Montanari, G. Raims, G. Busca, J. Catal. 228 (2004) 43.
[27] Ching-Huei Wang, Chemosphere 55 (2004) 11.
[28] Ruiguin Yang, Yilu Fu, Yi Zhang, Noritatsu Tsubaki, J. Catal 228 (2004) 23.
[29] T. Fujitani, J. Nakamura, Appl. Catal. A Gen. 191 (2000) 111.
[30] B. Dean, Clarkeand Alexis T. Bell, J. Catal. 154 (1995) 314.

[31] Yi Zhang, Ruiqin Yang, Noritatsu Tsubaki, J. Catal. 132 (2008) 93.
[32] Ruiqin Yang, Yi Zhang, Noritatsu Tsubaki, Catal. Commun. 6 (2008) 275.
[33] H. Shin-ichiro, Fujita, Masahito Usui, Hiroto Ito, Nobutsune Takezawa, J. Catal. 157 (1995) 403.
[34] K.C. Waugh, Catal. Today 15 (1992) 51.
[35] S. Fujita, M. Usui, H. Ito, N. Takezawa, J. Catal. 157 (1995) 403.
[36] I.A. Fisher, A.T. Bell, J. Catal. 178 (1998) 153.
[37] Qi Sun, Chong-Wei Liu, Wei Pan, Qi-Ming Zhu, Jing-Fa Deng, Appl. Catal. A 171 (1998) 301.
[38] B. Frank, F.C. Jentoft, H. Soerijanto, J. Kröhnert, R. Schlögl, R. Schomäcker, J. Catal. 246 (2007) 177.
[39] F. Le Peltier, P. Chaumette, J. Saussey, M.M. Bettahar, J.C. Lavalley, J. Mol. Catal. A Chem. 132 (1998) 91.
[40] D.B. Clarke, A.T. Bell, J. Catal. 154 (1995) 314.
[41] M. Bowker, R.A. Hadden, H. Houghton, J.N.K. Hyland, K.C. Waugh, J. Catal. 109 (1988) 263.